ChemMedChem

ResearchArticle
doi.org/10.1002/cmdc.202100739

Chemistry Europe
European Chemical Societies Publishing

www.chemmedchem.org

The Exception That Proves the Rule: How Sodium Chelation Can Alter the Charge-Cell Binding Correlation of Fluorescein-Based Multimodal Imaging Agents

Marco Maspero,[a, b] Clelia Dallanoce,[b] Björn Wängler,[c] Carmen Wängler[+],*[a] and Ralph Hübner[+]*[a]

In the present study we describe and explain an aberrant behavior in terms of receptor binding profile of a fluorescein-based multimodal imaging agent for gastrin releasing peptide receptor (GRPR) visualization by elucidating a chelating mechanism on sodium ions of its fluorescent dye moiety. This hypothesis is supported by both biological results and spectroscopic analyses of different fluorescein-carrying conjugates and an equally charged set of analogous tartrazine-based GRPR-binding imaging agents. Fluorescein interacts with sodium which reduces the overall negative charge of the dye molecule by one. This reduction in apparent total net charge explains the exceptional behavior found for the fluorescein-based multimodal bioconjugate in the context of the charge-cell binding correlation hypothesis.

Introduction

Recent studies[1–4] revealed that, when aiming to synthesize peptide-based dually labelled imaging probes suited for both positron emission tomography[5,6] and optical imaging[7,8] (PET/OI), the choice of the fluorescent dye for the optical detection can have a significant influence on the *in vitro* binding profile of the resulting multimodal imaging agent. At first, this was observed for dually labelled PESIN derivatives for gastrin-releasing peptide receptor (GRPR)-specific imaging (PESIN: PEG_3-BBN_{7-14}, BBN_{7-14}: truncated peptide sequence of the endogenous GRPR ligand bombesin, Figure 1), whose receptor affinities showed to be negatively affected by the introduction of negative charges being introduced by the respective fluorescent dye. Therefore, it was assumed that the higher the number of anionic charges carried by the conjugate (being determined by the fluorescent dye used), the lower the resulting GRPR binding affinity of the resulting multimodal imaging agent. This theory was confirmed upon various PESIN-monomer conjugates[1] presenting different dye units, as well as with the corresponding PESIN-homodimer[3,4] and -homotetramer[2] conjugates. By comparing the binding profiles within these series, it was also observed that the GRPR affinities of the conjugates carrying a higher number of peptide copies were less affected by the anionic charges of the introduced fluorescent dyes than their corresponding conjugates exhibiting a lower peptide valency. From this, the second assumption emerged that the adverse influence of negatively charged fluorescent dyes on the GRPR binding affinities of PESIN-based dually labeled imaging agents can be mitigated by a higher number of peptide copies. Both factors have thus to be taken into consideration during the design of tailored hybrid multimodal imaging agents.[9–11]

However, when expanding the palette of dually labeled hybrid multimodal peptide-based imaging agents, we came across a fluorescein-carrying PESIN monomer (**1a**, Figure 1) whose GRPR binding profile apparently did not fit to the previously described receptor binding data of comparable agents such as the respective peptide homodimer. This dually labeled agent was composed of PESIN and a multimodal imaging unit (MIU) carrying the fluorescein dye and a chelator for radiolabeling.

In the present study we describe and explain this aberrant behavior by elucidating a chelating mechanism on sodium ions of the fluorescein dye moiety of this dually labeled peptide monomer.

[a] *M. Maspero, Prof. Dr. C. Wängler,[+] Dr. R. Hübner[+]*
Biomedical Chemistry
Clinic of Radiology and Nuclear Medicine
Medical Faculty Mannheim of Heidelberg University
Theodor-Kutzer-Ufer 1–3, 68167 Mannheim (Germany)
E-mail: Carmen.Waengler@medma.uni-heidelberg.de
Ralph.Huebner@medma.uni-heidelberg.de
[b] *M. Maspero, Prof. C. Dallanoce*
Department of Pharmaceutical Sciences
Medicinal Chemistry Section "Pietro Pratesi"
University of Milan
Via L. Mangiagalli 25, 20133, Milan (Italy)
[c] *Prof. Dr. B. Wängler*
Molecular Imaging and Radiochemistry
Department of Clinical Radiology and Nuclear Medicine
Medical Faculty Mannheim of Heidelberg University
Theodor-Kutzer-Ufer 1–3, 68167 Mannheim (Germany)
[+] *Equal principal investigators and corresponding authors*

Supporting information for this article is available on the WWW under https://doi.org/10.1002/cmdc.202100739

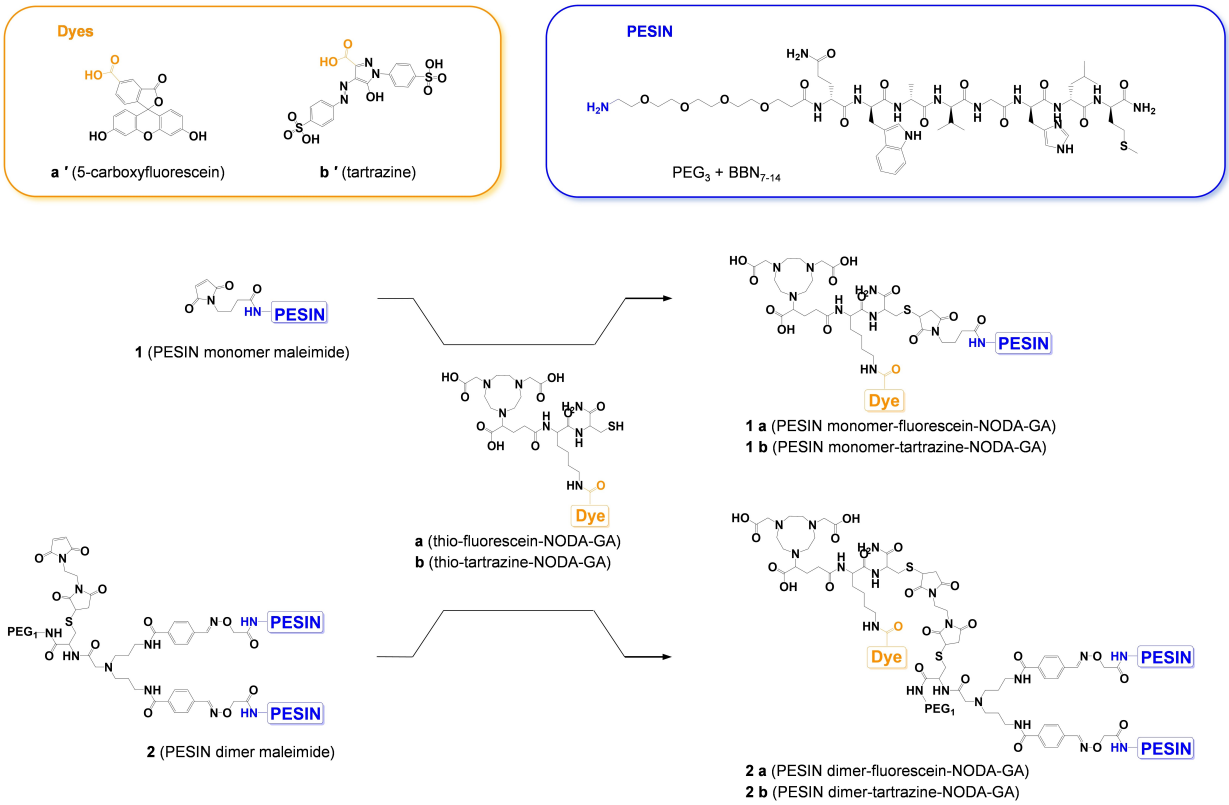

Figure 1. Schematic depiction of the structure and the synthesis of the multimodal imaging agents **1 a**, **2 a**, **1 b** and **2 b** from the multimodal imaging units **a** and **b** and the maleimide-modified PESIN monomer **1** and PESIN dimer **2**.

Results and Discussion

For the elucidation of the aberrant GRP receptor binding behavior of the newly developed hybrid multimodal GRPR-specific imaging agent **1 a**, different approaches were followed. One was the determination of the receptor affinities as determined by competitive displacement studies on GRPR-expressing HEK cells. The other one was based on spectroscopic analyses.

Moreover, a reference set of bioconjugates was synthesized and studied under the same conditions, comprising the dually negatively charged dye tartrazine instead of fluorescein (**1 b** and **2 b**, Figure 1). The two conjugates series (comprising either fluorescein or tartrazine) were prepared employing a previously described convergent synthetic strategy,[3] which reacts the receptor-specific mono- or divalent peptide moiety[12] with the respective fluorescent dye and chelator-bearing MIU.

Both tartrazine and fluorescein are well-known dyes, the first commonly used as pharmaceutical and food colorant,[13,14] while the second is a broadly used fluorescent probe in biological and biochemical applications.[15,16] Unlike tartrazine, fluorescein and its derivatives can exist in aqueous solution in a number of prototropic forms: cationic, neutral, monoanionic and di-anionic (Figure 2A). In particular, there are three different tautomers for the neutral species – a quinoid, a zwitterion and a neutral species – and a further two for the monoanion, with ionized carboxyl or hydroxyl groups.[17] As a result, the spectroscopic properties of fluorescein – such as absorption and fluorescence – are strongly pH dependent, and it was determined that to each proteolytic form of the dye molecule, a specific absorption spectrum is associated, with characteristic shape and absorption peaks (Figure 2B and Figure 3A).[18]

On these grounds, the equilibrium constants of fluorescein derivatives can be defined *via* spectroscopic analysis, as well as the fluorescein conformation at different pH values. For instance, when testing the GRPR affinities of compounds **1 a** and **2 a** (Figure 1), it is possible to determine that under the assay conditions, the fluorescent dye in the MIU of the hybrid conjugates exists prevalently in the di-anionic conformation.

This was demonstrated by analyzing the absorption spectra of the two compounds at the fixed pH value of the medium (measured pH of 8.23): both spectra presented main absorption peaks at 496/498 nm, with a shoulder around 475 nm, corresponding to the di-anionic proteolytic form of fluorescein, being in line with data reported in literature.[18] As confirmation, in the context of the charge-cell binding correlation, the PESIN dimer derivative **2 a** showed a GRPR binding affinity comparable to other dimeric PESIN conjugates carrying two anionic charges within the dye moiety,[2,3] including the tartrazine-based conjugate **2 b** being evaluated under the same conditions for direct comparison (IC_{50} values of 62.07 ± 3.87 nM and 58.44 ± 1.47 nM for **2 a** and **2 b**, respectively; Table 1). These results demonstrate a clear correlation between the number of negative charges

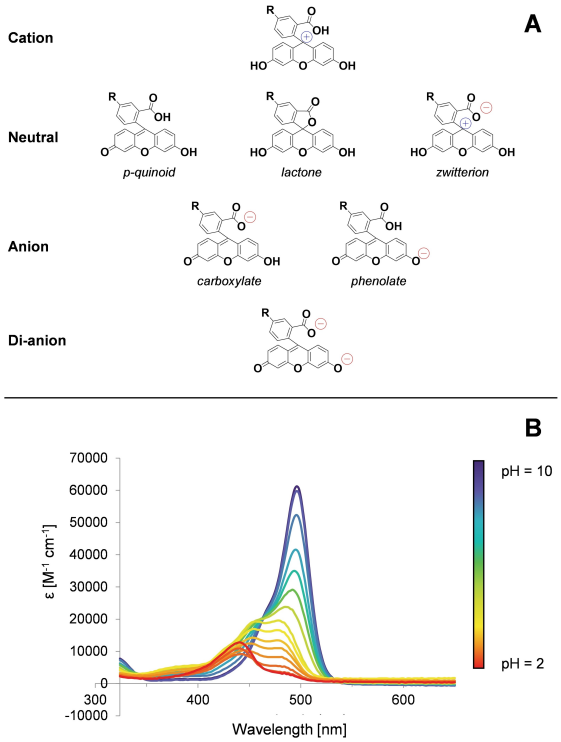

Figure 2. Proteolytic structures of fluorescein at different pH values of the solution (**A**); Absorption spectra of compound **1 a** (10 μM) in pure water, recorded at pH 9.8, 9.2, 8.0, 7.5, 7.0, 6.7, 6.2, 5.3, 4.6, 4.2, 3.9, 3.5, 3.0, 2.3 and 2.0 (**B**).

carried by the dye molecule within multimodal imaging agent and its GRPR binding properties.

In contrast, the IC_{50} value of the monomeric fluorescein-bearing PESIN conjugate **1 a** (60.33 ± 3.53 nM) diverged significantly from the one of the tartrazine-based counterpart **1 b** (117.00 ± 3.71 nM), although both compounds are characterized by two anionic charges within their dye moiety. Interestingly, the GRPR binding affinity of **1 a** is better comparable to those which were reported for analogous agents carrying mono-anionic dyes.[1] Thus, the fluorescein dye in **1 a** seems to be present in the mono-anionic instead of the di-anionic conformation. This apparently aberrant behavior is explainable assuming a previously undescribed mechanism of chelation of sodium ions by fluorescein. Interactions of fluorescein derivatives with metal ions have been reported in literature and exploited for their application as fluorescent chemosensors for the detection of both cations and anions.[19–22] The binding mode proposed in this work consists of an interaction between the phenolic and the carboxylic group of fluorescein and one sodium ion (Figure 4A). As a result, the introduction of a positively charged metal ion in the predicted proteolytic conformation of the fluorescein moiety can entail a masking of one anionic group and a reduction of the total net charge of compound **1 a**, explaining its unexpected GRPR binding behavior.

In addition to the binding affinity results, this hypothesis is supported by the spectroscopic analysis of the fluorescein-based conjugates. Figure 3A shows absorption spectra of compounds **1 a** and **2 a** recorded in the pH range of 2–9 in 0.1 M NaCl solution (being the sodium concentration in the binding affinity assay medium[23]). Unlike the fluorescein analysis methods reported in literature,[17,18,24] this titration was performed without the use of buffer solutions, instead only hydrochloric acid and ammonia solutions were used. Moreover, these analyses were conducted both in presence and in

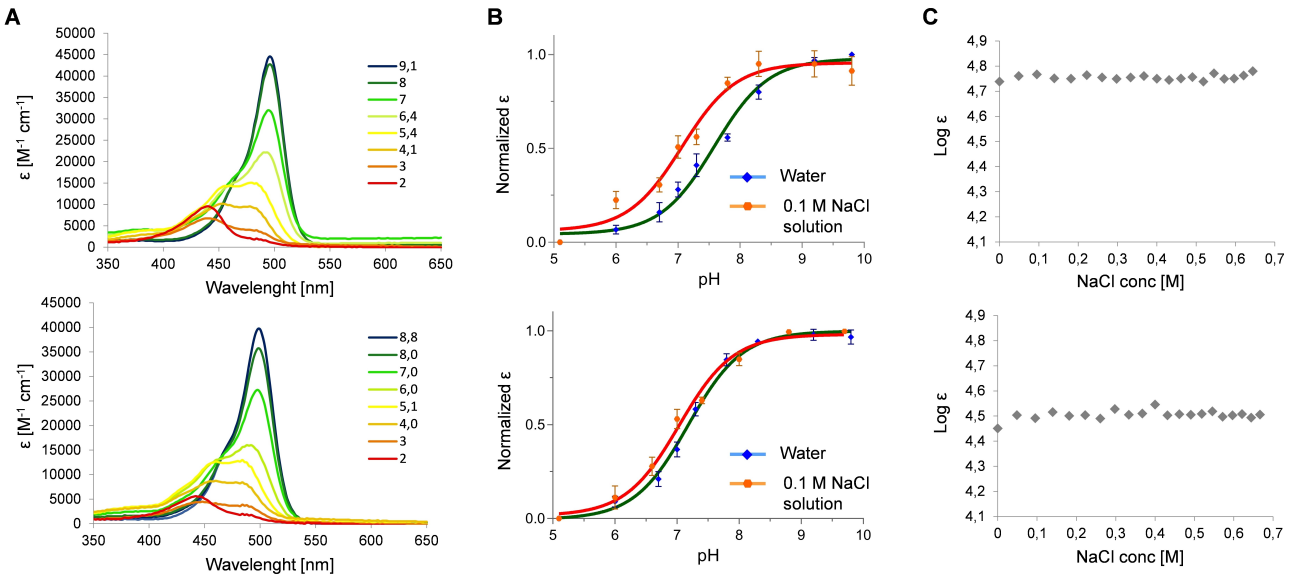

Figure 3. Absorption spectra of **1 a** (top) and **2 a** (bottom) 10 μM in 0.1 M NaCl solution, recorded at different pH values (**A**); Normalized variation of molar absorptivity in relation to pH of **1 a** (top) and **2 a** (bottom) in pure water (blue) and in 0.1 M NaCl solution (orange). Errors are given as ± SD and values were obtained in three different experiments, each performed in triplicate (**B**); Molar absorptivity in relation to NaCl concentration of **1 a** (top) and **2 a** (bottom) recorded at pH 8.23 (**C**).

Table 1. Summary of the $log_{D(7.4)}$ values and the GRPR affinity data (IC_{50} values), all given as mean ± SD and obtained in three different experiments, each performed in triplicate, of the hybrid conjugates **1a** and **2a and 1b** and **2b**, as well as their photophysical properties determined in pure water at a concentration of 1×10^{-5} mol L^{-1}.

Compound	IC_{50} [a] [nM]	$log_{D(7.4)}$	$\lambda_{max(abs)}$ [b] [nm]	log ε [$M^{-1}cm^{-1}$]	$\lambda_{max(em)}$ [c] [nm]
1a	60.33 ± 3.53	-3.27 ± 0.02	496	4.72	523
1b	62.07 ± 3.87	-2.54 ± 0.06	498	4.59	525
2a	117.00 ± 3.71	-3.58 ± 0.02	432	4.09	-
2b	58.44 ± 1.47	-2.23 ± 0.06	440	4.17	-

[a] Competitive displacement studies performed on a stably GRPR-transfected HEK-293 cell line. [b] Spectra were recorded in deionized water at pH 8.23. [c] excitation wavelength λ_{ex}: 400 nm.

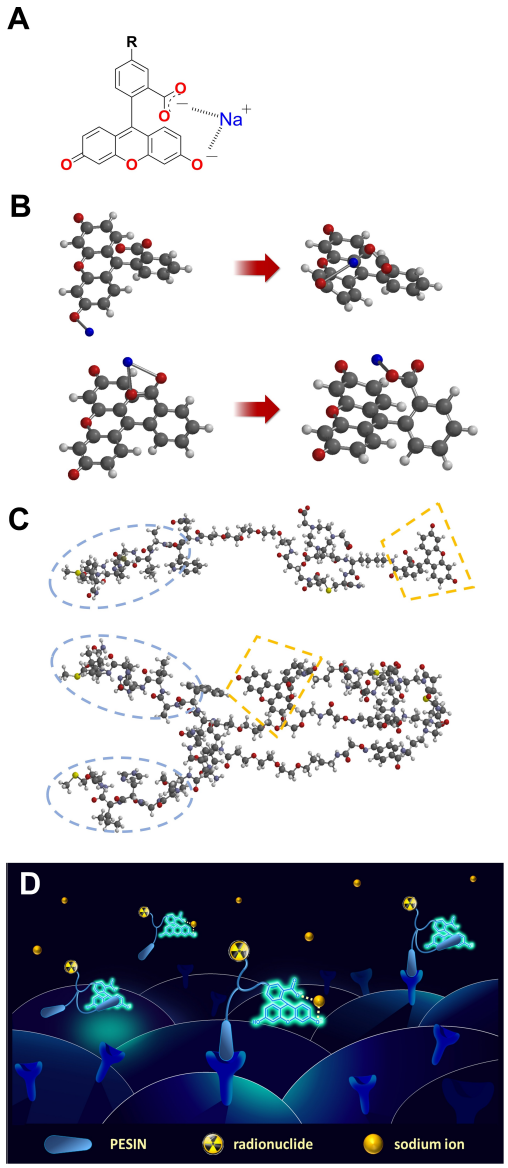

Figure 4. Proposed chelation mode between the di-anionic conformation of fluorescein and sodium (**A**); starting points and DFT minimized energy structures of fluorescein phenolate (top) and carboxylate (bottom) sodium salts (**B**); Molecular mechanics minimized energy structures of **1a** (top) and **2a** (bottom) with highlighted PESIN moieties (light blue) and fluorescein dye (yellow) (**C**); Graphical representation of the PESIN monomer-MIU conjugate (**1a**) and the PESIN dimer-MIU conjugate (**2a**) interacting with the GRP receptor in presence of sodium ions (**D**).

complete absence of sodium salts, to highlight the influence of this metal ion on the proteolytic equilibria.

The results demonstrate that, while compound **2a** does not present any significant variation, the presence of sodium in the titration experiment of **1a** has a clear impact on the mono-/di-anionic equilibrium. As shown in Figure 3B, the addition of the metal ion alters the molar absorptivity (ε) variation in the pH range of 5–10, indicating a decrease in the value of the mono-/di-anion proteolytic constant. This alteration is due to the stabilization of the di-anionic conformation of fluorescein, determined by the previously described chelating mechanism with sodium ions. Furthermore, to exclude the increase of ionic strength as a potential cause of this variation, a sodium titration at fixed pH (pH 8.23) was performed, revealing that the increment in NaCl concentration does not result in a significant variation of absorptivity for neither compound **1a** nor **2a** (Figure 3C).

Taken together, these results imply that the sodium chelation takes place both when **1a** is in solution or when interacting with its target receptor, explaining its unexpectedly high affinity for the GRPR as determined in the competitive receptor binding assays.

Additionally, to investigate the interaction position of the sodium ion within the structure of fluorescein, DFT calculations were performed. In detail, from the energy-minimized structures of both fluorescein phenolate and carboxylate sodium salts, it was observed that the metal salt ends up in the nearly same position in both simulations, between the carboxylate and the phenolate groups (Figure 4B). This suggests an interaction of both these functional groups with the sodium cation, making the described position the most appropriate to represent the chelation mechanism of sodium by the fluorescein molecule.

Although these results and explanations are well-suited to describe the aberrant behavior of **1a**, the same effect does not apply to the PESIN homodimer derivative **2a**. In this latter case, in fact, the presence of sodium does not alter either the photophysical characteristics or the GRPR affinity profile of the conjugate. This distinct difference can be explained by the potential interaction of the MIU with one of the peptidic copies of the PESIN homodimer, which can take place during the binding of the second peptide binder with the receptor as well as when the hybrid compound is in solution (Figure 4D).

This interaction is enabled by the complex and flexible structure of the dually labeled peptide homodimer, allowing intramolecular interactions between the fluorescent dye and one of the peptide copies (Figure 4C). Such flexibility is not present in the more simple and thus compact structure of the corresponding PESIN monomer. As a result, the cell binding properties of **2 a** are unaffected by the presence of sodium ions, so in line with the charge-cell binding correlation as described in the study which firstly reported this molecule.[3]

Conclusion

The introduction of the sodium chelation mechanism allows to explain the results obtained for the multimodal fluorescein-based PESIN derivative and the viability of the theory has been explored and explained using different approaches, which led to results being consistent with each other.

Although different behaviors can be expected when applying the studied multimodal imaging agents under *in vivo* conditions, it is safe to say that their *in vitro* GRPR affinity is strictly dependent on their total net charge. Compound **1 a** showed initially an unexpectedly high binding activity, being however explainable by the found interaction with sodium, making it the exception that proves the rule of the charge-cell binding correlation.

Experimental Section

Materials and instruments. All commercially available chemicals and solvents were at least of analytical grade and used, if not otherwise stated, without further purification. Fmoc-protected amino acids, Benzotriazole-1-yl-oxy-*tris*-pyrrolidino-phosphonium hexafluorophosphate (PyBOP) and Rink Amide resin (loading 0.54 mmol/g) were purchased form NovaBiochem (Darmstadt, Germany). 15-(9-Fluorenylmethyloxycarbonyl)amino-4,7,10,13-tetraoxa-pentadecanoic acid (PEG_3, Fmoc-NH-PEG_3-COOH), 8-(9-fluorenylmethyloxycarbonyl-amino)−3,6-dioxaoctanoic acid (PEG_1, Fmoc-NH-PEG_1-COOH), *N*-alpha-(9-fluorenylmethyloxycarbonyl)-S-(*t*Bu-thio)-*D*-cysteine (Fmoc-*D*-Cys(S−S-*t*Bu)-OH), {[*bis*(*t*-butyloxycarbonyl)amino]oxy}acetic acid monohydrate ($(Boc)_2$AOAc-OH × H_2O) and 2-(*bis*(3-(((9*H*-fluoren-9-yl)methoxy)carbonylamino)propyl)amino)acetic acid potassium hemisulfate (Fmoc-NH-Propyl)$_2$Gly-OH × $KHSO_4$) were obtained from Iris Biotech (Marktredwitz, Germany). *N*-succinimidyl-4-formylbenzoate (95 %) (SFB) and 4-maleimidobutyric acid were obtained from ABCR (Karlsruhe, Germany), and 4-(4,7-*bis*(2-(t-butoxy)−2-oxoethyl)−-1,4,7-triazacyclononan-1-yl)−5-(*tert*-butoxy)−5-oxopentanoic acid ((*R*)-NODA-GA(tBu)$_3$) from CheMatech (Dijon, France). *Tris*(2-carboxyethyl)phosphine hydrochloride (TCEP) was purchased from Alfa Aesar (Kandel, Germany), and 1,2-*bis*(maleimido)ethane (BME) and *tetrakis*(triphenylphosphine)palladium(0) ($Pd(PPh_3)_4$) from TCI (Eschborn, Germany). Morpholine, *N*,*N*-diisopropylethylamine (DIPEA), triisopropylsilane (TIS), 5(6)-carboxyfluorescein *N*-hydroxysuccinimide ester, ascorbic acid and tartazine were obtained from Sigma-Aldrich (Taufkirchen, Germany). Dichloromethane (DCM), diethylether, dimethylformamide (DMF), 2-(1*H*-benzotriazol-1-yl)−-1,1,3,3-tetramethyluronium hexafluoro-phosphate (HBTU), trifluoroacetic acid (TFA) and deionized water were purchased from Carl Roth (Karlsruhe, Germany), acetonitrile (MeCN) from Häberle Labortechnik (Lonsee-Ettlenschieß, Germany). For HPLC chromatography, a Dionex UltiMate 3000 system was used together with Chromeleon Software (Version 6.80). For semipreparative analyses, a Chromolith (RP-18e, 100–10 mm, Merck, Germany) column was used. For radioanalytical use, a Dionex UltiMate 3000 system equipped with a Raytest GABI Star radioactivity detector was used together with a Chromolith Performance (RP-18e, 100–4.6 mm, Merck, Germany) column. All operations were performed with a flow rate of 4 mL/min using H_2O + 0.1 % TFA and MeCN + 0.1 % TFA as solvents. HR-ESI (high-resolution Electrospray Ionization) and MALDI (Matrix-Assisted Laser Desorption/Ionization) mass analyses were carried out on a Thermo Finnigan LTQ FT Ultra Fourier Transform Ion Cyclotron Resonance (Dreieich, Germany) and a Bruker Daltronics Microflex spectrometer (Bremen, Germany), respectively. γ-counting was performed using a 2480 Wizard gamma counter system from Perkin Elmer (Rodgau, Germany). For pH measurements, a SevenMulti from Mettler Toledo (Gießen, Germany) was used. The absorbance measurements were performed on a Genesys 50 UV/Vis spectrophotometer from ThermoFisher (Dreieich, Germany), while the emission spectra were recorded on a Tecan Infinite M200 Microplate reader together with a Nunc Micro-Well 96 solid plate from ThermoFisher. Transfected Human Embryonic Kidney 293 cells stably expressing the GRP Receptor (HEK-GRPR) were obtained from Dr. Martin Béhé, Paul Scherrer Institute, Villingen, Switzerland. [^{125}I]I-Tyr^4-bombesin was purchased from Perkin Elmer (Rodgau, Germany) in a molar activity of 81.4 GBq/μmol. Dulbecco's Modified Eagle's Medium (DMEM, high glucose, GlutaMax-I, 500 mL), geneticin (G418 Sulfate, 50 mg/mL), Opti-MEM I (GlutaMAX I), RPMI 1640 medium, L-Glutamine and PenStrep were obtained from Gibco (Schwerte, Germany), FCS (fetal calf serum) from Bio&SELL (Feucht, Germany) and Dulbecco's phosphate buffered saline (PBS), and 0.25 % Trypsin with 0.02 % EDTA solution in PBS from Sigma-Aldrich (Taufkirchen, Germany). Bovine serum albumin (BSA) and sodium chloride (NaCl) were purchased from CarlRoth (Karlsruhe, Germany). The ^{68}Ge/^{68}Ga-Generator used was an IGG100 system, obtained from Eckert & Ziegler (Berlin, Germany) and eluted with HCl (0.1 M, 1.6 mL).

General synthesis of peptides. Peptides were synthesized on a Rink Amide resin by using N_α-Fmoc protecting groups and a standard HBTU activation strategy.[25] The resin was swollen in DCM for 30 min, washed with DMF, the Fmoc protecting group was cleaved with piperidine (50 % in DMF, 2 min washing then 5 min). The resin was washed with DMF, then the respective protected amino acid was coupled by using the HBTU-pre-activated synthon in DMF (4 equiv. N_α-Fmoc amino acid, 3.9 equiv. HBTU, 4 equiv. DIPEA) which was allowed to react for 2 min before being added to the resin. The syringe was shaken for 1 h, then the reaction mixture was removed and the resin was washed with DMF. The same procedure was repeated for the following amino acids. Detailed syntheses and analytical data of the PESIN peptide monomer **1** and dimer **2** can be found in the corresponding references.[1,3] Then the resin was washed thrice with DMF, dichloromethane and diethyl ether, and dried under reduced pressure. Finally, the peptides were cleaved from solid support by using a mixture of TFA:TIS (95 : 5 (v/v), 5 mL) for 1 h. The volatile components were removed under reduced pressure, the residues were dissolved in 1 : 1 MeCN:H_2O + 0.1 % TFA and the products purified by semipreparative HPLC.

General synthesis of the multimodal imaging units (MIUs) a and b. Rink amide resin-Cys(Trt)-Lys(alloc)-NODA-GA(tBu)$_3$ was synthesized according to the standard Fmoc-based solid phase peptide synthesis protocol reported earlier, then the allyloxycarbonyl protecting group was removed still on solid support using tetrakis(triphenylphosphine)palladium(0). In the following step, 50 μmol Rink amide resin-Cys(Trt)-Lys-NODA-GA(tBu)$_3$ was reacted with the respective dye **a**′ and **b**′. MIU **a**: 4 eq. of 5-carboxyfluorescein (**a**′) were activated beforehand with HBTU (3.8 eq.) and

DIPEA (4 eq.) as base in DMF (4 mL) for 2 minutes, then reacted with the resin for 1 hour. MIU **b**: 2 eq. of tartrazine (**b'**) were activated beforehand with PyBOP (1.9 eq.) and DIPEA (2 eq.) as base in DMF (3 mL) for 2 minutes, then reacted with the resin at 80 °C for 4 hours. After the conjugation reactions were finished, the resin was filtered from the liquid components of the mixture and washed thrice with DMF, dichloromethane and diethyl ether. After drying, the dye conjugates were cleaved from solid support by using a mixture of TFA:TIS (95 : 5 (v/v), 5 mL) for 1–2 h. Then the volatile components were removed under reduced pressure, the residues were dissolved in 1 : 1 MeCN:H_2O + 0.1 % TFA and the products purified by semipreparative HPLC. Analytical data of **a** and **b**: **a**: ($C_{45}H_{53}N_9O_7S$): HPLC gradient (analytical): 0–100 % MeCN + 0.1 % TFA in 12 min, R_t = 5.80 min, yield: 30 %, purity: 97 %, MALDI-MS (m/z) for $[M+H]^+$ (calculated): 964.26 (964.34); $[M+Na]^+$ (calculated): 986.28 (986.32); $[M+K]^+$ (calculated): 1002.25 (1002.30); HR-ESI-MS (m/z) for $[M+H+Na]^{2+}$ (calculated): 493.2250 (493.2509). (HPLC, ESI and MALDI characterizations are reported in a previous paper[3]). **b**: ($C_{40}H_{53}N_{11}O_{17}S_3$): HPLC gradient (analytical): 0–55 % MeCN + 0.1 % TFA in 15 min, R_t = 6.28 min, yield: 10 %, purity: 98 %, MALDI-MS (m/z) for $[M+H]^+$ (calculated): 1057.44 (1057.10); $[M+Na]^+$ (calculated): 1079.41 (1079.09); $[M+K]^+$ (calculated): 1095.33 (1095.20); HR-ESI-MS (m/z) for $[M+2Na]^{2+}$ (calculated): 553.0879 (553.1298).

General synthesis of the peptide-MIU-conjugates 1 a, 2 a, 1 b and 2 b. 1.45 μmol of the respective peptide (1 eq.) and 1.60 μmol of the respective MIU (1.1 eq.) were dissolved in 200 μL of 1 : 1 MeCN: H_2O + 0.1 % TFA and the pH was adjusted to 7.0 using phosphate buffer (0.5 M, pH 7.2). After 5 minutes of reaction at 25 °C, the HPLC purification of the products was performed. Analytical data for **1 a**, **2 a**, **1 b** and **2 b**: **1 a** ($C_{107}H_{144}N_{22}O_{32}S_2$): HPLC gradient: 0–100 % MeCN + 0.1 % TFA in 12 min, R_t = 6.00 min, yield: 67 %, purity: 98 %, MALDI-MS (m/z) for $[M+H]^+$ (calculated): 2315.62 (2315.68); $[M+Na]^+$ (calculated): 2338.05 (2338.06); HR-ESI-MS (*m/z*) for $[M+3Na]^{3+}$ (calculated): 796.5123 (796.5423). **2 a**: ($C_{200}H_{279}N_{45}O_{58}S_4$): HPLC gradient: 0–100 % MeCN + 0.1 % TFA in 12 min, R_t = 6.50 min, yield: 30 %, purity: 99 %, MALDI-MS (m/z) for $[M+H]^+$ (calculated): 4368.06 (4367.92); $[M+Na]^+$ (calculated): 4390.68 (4389.90); $[M+K]^+$ (calculated): 4406.18 (4405.89); HR-ESI-MS (m/z) for $[M+H+3Na]^{4+}$ (calculated): 1109.2219 (1109.2230). (HPLC, ESI and MALDI characterizations are reported in a previous paper[3]). **1 b**: ($C_{102}H_{146}N_{26}O_{34}S_4$): HPLC gradient: 0–100 % MeCN + 0.1 % TFA in 8 min, R_t = 4.47 min, yield: 42 %, purity: 99 %, MALDI-MS (m/z) for $[M+H]^+$ (calculated): 2409.56 (2409.68); $[M+Na]^+$ (calculated): 2432.56 (2432.68); $[M+K]^+$ (calculated): 2448.14 (2448.68); HR-ESI-MS (*m/z*) for $[M+Na+K]^{2+}$ (calculated): 1235.4218 (1235.3841). **2 b**: ($C_{107}H_{144}N_{22}O_{32}S_2$): HPLC gradient: 0–100 % MeCN + 0.1 % TFA in 12 min, R_t = 6.00 min, yield: 76 %, purity: 98 %, MALDI-MS (m/z) for $[M+H]^+$ (calculated): 4463.73 (4463.02); $[M+Na]^+$ (calculated): 4486.18 (4486.00); $[M+K]^+$ (calculated): 4502.11 (4502.12); HR-ESI-MS (*m/z*) for $[M+H+2Na]^{3+}$ (calculated): 1502.9456 (1502,9998).

Radiochemistry. A solution of 5 nmol of the MIUs or the peptide-MIU-conjugates in H_2O (Tracepur quality, 1 mM) was added to 90–120 MBq of [^{68}Ga]$GaCl_3$ in a solution obtained by fractioned elution of an IGG ^{68}Ge/^{68}Ga generator system with HCl (0.1 M, 1.6 mL) and subsequent titration to pH 3.5–4.2 by addition of sodium acetate solution (1.25 M, 50–75 μL). All labeling experiments were performed by addition of 1 mg ascorbic acid to suppress radiolysis-induced product fragmentation. In the labelling experiments of **a** and **b**, 1 mg TCEP × HCl was also added. After 10 minutes of reaction at 45 °C, the mixtures were analyzed by analytical radio-HPLC. The radiolabeled products were found to be 95–99 % pure and obtained in non-optimized molar activities of 90–120 GBq/μmol. The only exception from is was [^{68}Ga]Ga-**b** which could only be obtained in a radiochemical purity of 82 % due to side reactions of the free thiol functionality under labeling conditions.

$Log_{D(7.4)}$ determination. The water/1-octanol partition coefficient ($log_{D(7.4)}$) was determined by adding 5 μL of the respectively ^{68}Ga-labeled compound (0.8–1.2 MBq) in aqueous solution to a mixture of phosphate buffer (0.05 M, pH 7.4, 795 μL) and 1-octanol (800 μL). The mixtures were intensively shaken for 5 minutes on a vibrating plate. After subsequent centrifugation at 13,000 rpm for 5 min, 125 μL were taken from each phase and measured in a γ-counter. The $log_{D(7.4)}$ values were calculated from three or four independent experiments, each performed in triplicate.

***In vitro* competitive binding assays**. Stably GRPR-transfected Human Embryonic Kidney 293 cells (HEK-GRPR) were cultured at 37 °C in Dulbecco's Modified Eagle's Medium (DMEM, high glucose, GlutaMax-I, 500 mL) supplemented with 10 % FCS (50 mL), 1.5 % Geniticin (8.25 mL) and 1 % PenStrep (5.5 mL) in a humidified atmosphere containing 5 % CO_2. The medium was exchanged every two or three days and cells were split at > 75 % confluence. To determine the *in vitro* binding affinities, competitive displacement studies were performed and each compound was evaluated at least three times, each experiment being performed in triplicate. A Millipore Multiscreen punch kit and Millipore 96 well filter plates (pore size 1.2 μm) were used. The plates were incubated with PBS/BSA (1 %) solution (each well 200 μL) at 25 °C for one hour before use. The dilution series of the conjugates (0.5–1000 nM for **1 a, 1 b** and **2 b**, 0.25–500 nM for **2 a**), and the reference compound BBN (0,1–250 nM) were prepared in the binding buffer. The solution of the GRPR-specific radioligand [^{125}I]I-Tyr^4-bombesin was prepared by adding 55–75 kBq of this agent to 7 mL of binding buffer. The HEK-GRPR cells were harvested and re-suspended in the binding buffer to give a cell concentration of 2×10^6 cells/mL. After the BSA solution was filtered using the Millipore Multiscreen vacuum manifold, 50 μL of a cell suspension containing 10^5 cells were seeded in each well. Subsequently, 25 μL of the ^{125}I-labeled agent solution (0.01 kBq/μL) and 25 μL of the compound to be tested were added. The substances were added in eleven increasing concentrations, while the 12th well contained no test compound to ensure the 100 % binding of the ^{125}I-labeled competitor. After incubation of the plate for another hour at 25 °C, the solution was filtrated, and the cells were washed three times with cold PBS (1 × 200 μL, 2 × 100 μL). Using a Millipore MultiScreen disposable punch and a Millipore MultiScreen punch kit, the filters of the well plate were collected in γ-counter tubes separately and measured by γ-counting. The determination of the half-maximal inhibitory concentration (IC_{50}) values was performed by fitting the obtained data via nonlinear regression using GraphPad Prism (v5.01).

pH and sodium titrations of compounds 1 a and 2 a. For the pH titration in pure water, a solution of compounds **1 a** and **2 a** in deionized water (10 μM, 5 mL) was basified with 100 μL of ammonia solution (0.1 M) to pH ≈ 10. The basic solution was then treated with consecutive additions of 2 μL HCl solution (0.1 M) to pH 2. After each addition, the absorption spectra were recorded. The pH titration in presence of sodium was performed as previously described for the titration in pure water by addition of NaCl in a concentration of 0.1 M in both the 10 μM solution of compounds **1 a** and **2 a** and the 0.1 M titrating solutions of ammonia and HCl. For the sodium titration, the pH of a solution of compounds **1 a** and **2 a** in deionized water (10 μM, 5 mL) was adjusted to pH 8.23 using ammonia and HCl solutions (0.1 M). The resulting solution was then treated with 20 consecutive additions of 150 μL NaCl solution (2 M). After each addition, the pH was corrected to the value of 8.23 and the absorption spectra were recorded.

DFT calculations. DFT calculations were conducted as implemented in Spartan'20 (1.0.0)[26] using B3LYP[27–29] exchange correlation func-

tionals and 6–31G* polarization basis set were assigned for all elements. Characterization of each optimized structure as local minimum on the potential energy surface was carried out by harmonic frequency analysis based on the second derivative. Start geometries for the structure optimization were taken from the library implemented in Spartan. The structures (Monoanionic phenolate and monoanionic carboxylate) were subsequently optimized in Spartan and the local minima determined, then the proton was exchanged by a sodium atom and the structure was minimized again and after the local minima determined. The bioconjugates (monomer and dimer) were constructed from a DFT minimized structure of BBN_{7-14} and DFT minimized structure of the MIU and then the energy was minimized only by the molecular mechanics minimization implemented in Spartan. All attempts to calculate the energy minimum by DFT failed because of the size of the molecules.

Acknowledgements

We would like to thank Werner Spahl (LMU Munich) for performing HR-ESI-MS measurements and Martin Béhé (Paul Scherrer Institute, Villingen, Switzerland) for providing the stably GRPR-transfected HEK-293 cells. Open Access funding enabled and organized by Projekt DEAL.

Conflict of Interest

The authors declare no conflict of interest.

Data Availability Statement

The data that support the findings of this study are available in the supplementary material of this article.

Keywords: charge-cell binding correlation · fluorescein · multimodal imaging · radiochemistry · receptors · sodium chelation · tartrazine

[1] M. Maspero, X. Cheng, V. von Kiedrowski, C. Dallanoce, B. Wängler, R. Hübner, C. Wängler, *Pharmaceuticals* **2021**, *14*, 989.
[2] R. Hübner, A. Paretzki, V. von Kiedrowski, M. Maspero, X. Cheng, G. Davarci, D. Braun, H. Damerow, B. Judmann, V. Filippou, C. Dallanoce, R. Schirrmacher, B. Wängler, C. Wängler, *Pharmaceuticals* **2021**, *14*, 531–545.
[3] R. Hübner, X. Cheng, B. Wängler, C. Wängler, *Chem. Eur. J.* **2020**, *26*, 16349–16356.
[4] R. Hübner, V. von Kiedrowski, V. Benkert, B. Wängler, R. Schirrmacher, R. Krämer, C. Wängler, *Pharmaceuticals* **2020**, *13*, 250–264.
[5] T. Derlin, V. Grünwald, J. Steinbach, H. J. Wester, T. L. Ross, *Dtsch. Arztebl. Int.* **2018**, *115*, 175–181.
[6] L. G. Marcu, L. Moghaddasi, E. Bezak, *Int. J. Radiat. Oncol. Biol. Phys.* **2018**, *102*, 1165–1182.
[7] V. von Kiedrowski, R. Hübner, D. Kail, R. Schirrmacher, C. Wängler, B. Wängler, *J. Mater. Chem. B* **2020**, *8*, 10602.
[8] C. Wang, Z. Wang, T. Zhao, Y. Li, G. Huang, B. D. Sumer, J. Gao, *Biomaterials* **2017**, *157*, 62–75.
[9] J. Rieffel, U. Chitgupi, J. F. Lovell, *Small* **2015**, *11*, 4445–4461.
[10] D. Ni, E. B. Ehlerding, W. Cai, *Angew. Chem. Int. Ed.* **2019**, *58*, 2570–2579; *Angew. Chem.* **2019**, *131*, 2592–2602.
[11] U. Seibold, B. Wängler, R. Schirrmacher, C. Wängler, *BioMed Res. Int.* **2014**, *2014*, 1–13.
[12] R. Hübner, V. Benkert, X. Cheng, B. Wängler, R. Krämerb, C. Wängler, *J. Mater. Chem. B* **2020**, *8*, 1302.
[13] M. Lee, A. F. Gentry, R. Schwartz, J. Bauman, *Drug Intell. Clin. Pharm.* **1981**, *15*, 782–788.
[14] K. Rovina, S. Siddiquee, S. M. Shaarani, *Crit. Rev. Anal. Chem.* **2017**, *47*, 309–324.
[15] F. Acerbi, C. Cavallo, M. Broggi, R. Cordella, E. Anghileri, M. Eoli, M. Schiariti, G. Broggi, P. Ferroli, *Neurosurg. Rev.* **2014**, *37*, 547–557.
[16] F. Le Guern, V. Mussard, A. Gaucher, M. Rottman, D. Prim, *Int. J. Mol. Sci.* **2020**, *21*, 9217–9240.
[17] V. Zanker, W. Peter, *Chem. Ber.* **1957**, *91*, 572–580.
[18] R. Sjöback, J. Nygren, M. Kubista, *Spectrochim. Acta Part A* **1995**, *51*, L7–L21.
[19] K. M. K. Swamy, S.-K. Ko, S. K. Kwon, H. N. Lee, C. Mao, J.-M. Kim, K.-H. Lee, J. Kim, I. Shin, J. Yoon, *Chem. Commun.* **2008**, *45*, 5915–5917.
[20] S. C. Burdette, G. K. Walkup, B. Spingler, R. Y. Tsien, S. J. Lippard, *J. Am. Chem. Soc.* **2001**, *123*, 7831–7841.
[21] P. Zhang, C. Li, H. Zhang, Y. Li, X. Yu, X. Geng, Y. Wang, X. Zhen, Z. Ma, *J. Inclusion Phenom. Macrocyclic Chem.* **2014**, *81*, 295–300.
[22] A. Minta, J. P. Y. Kao, R. Y. Tsien, *J. Biol. Chem.* **1989**, *264*, 8171–8178.
[23] The complete formulation of the OPTIMEM assay medium is proprietary, thus a partial disclosure of the sodium content was obtained from direct correspondence with ThermoFisher Scientific.
[24] E. W. Emmart, *Arch. Biochem. Biophys.* **1958**, *73*, 1–8.
[25] D. A. Wellings, E. Atherton, *Methods Enzymol.* **1997**, ***289***, 44–67.
[26] Y. Shao, L. F. Molnar, Y. Jung, J. Kussmann, C. Ochsenfeld, S. T. Brown, A. T. B. Gilbert, L. V. Slipchenko, S. V. Levchenko, D. P. O'Neill, R. A. DiStasio, R. C. Lochan, T. Wang, G. J. O. Beran, N. A. Besley, J. M. Herbert, C. Y. Lin, T. Van Voorhis, S. H. Chien, A. Sodt, R. P. Steele, V. A. Rassolov, P. E. Maslen, P. P. Korambath, R. D. Adamson, B. Austin, J. Baker, E. F. C. Byrd, H. Dachsel, R. J. Doerksen, A. Dreuw, B. D. Dunietz, A. D. Dutoi, T. R. Furlani, S. R. Gwaltney, A. Heyden, S. Hirata, C. P. Hsu, G. Kedziora, R. Z. Khalliulin, P. Klunzinger, A. M. Lee, M. S. Lee, W. Liang, I. Lotan, N. Nair, B. Peters, E. I. Proynov, P. A. Pieniazek, Y. M. Rhee, J. Ritchie, E. Rosta, C. D. Sherrill, A. C. Simmonett, J. E. Subotnik, H. L. Woodcock, W. Zhang, A. T. Bell, A. K. Chakraborty, D. M. Chipman, F. J. Keil, A. Warshel, W. J. Hehre, H. F. Schaefer, J. Kong, A. I. Krylov, P. M. W. Gill, M. Head-Gordon, *Phys. Chem. Chem. Phys.* **2006**, *8*, 3172–3191.
[27] P. J. Stephens, F. J. Devlin, C. F. Chabalowski, M. J. Frisch, *J. Phys. Chem.* **1994**, *98*, 11623–11627.
[28] A. D. Becke, *Phys. Rev. A* **1988**, *38*, 3098–3100.
[29] C. T. Lee, W. T. Yang, R. G. Parr, *Phys. Rev. B* **1988**, *37*, 785–789.

Manuscript received: December 30, 2021
Revised manuscript received: February 7, 2022
Accepted manuscript online: February 9, 2022
Version of record online: February 22, 2022